



# GSK3 $\beta$ -Dependent Phosphorylation Alters DNA Binding, Transactivity and Half-Life of the Transcription Factor USF2

Tina Horbach<sup>1,2</sup>, Tabughang Franklin Chi<sup>1</sup>, Claudia Götz<sup>3</sup>, Satyan Sharma<sup>1</sup>, André H. Juffer<sup>1</sup>, Elitsa Y. Dimova<sup>1</sup>, Thomas Kietzmann<sup>1\*</sup>

**1** Faculty of Biochemistry and Molecular Medicine, Biocenter Oulu, University of Oulu, Oulu, Finland, **2** Department of Chemistry, University of Kaiserslautern, Kaiserslautern, Germany, **3** Medical Biochemistry and Molecular Biology, Saarland University, Homburg, Germany

## Abstract

The upstream stimulatory factor 2 (USF2) is a regulator of important cellular processes and is supposed to have also a role during tumor development. However, the knowledge about the mechanisms that control the function of USF2 is limited. The data of the current study show that USF2 function is regulated by phosphorylation and identified GSK3 $\beta$  as an USF2-phosphorylating kinase. The phosphorylation sites within USF2 could be mapped to serine 155 and threonine 230. In silico analyses of the 3-dimensional structure revealed that phosphorylation of USF2 by GSK3 $\beta$  converts it to a more open conformation which may influence transactivity, DNA binding and target gene expression. Indeed, experiments with GSK3 $\beta$ -deficient cells revealed that USF2 transactivity, DNA binding and target gene expression were reduced upon lack of GSK3 $\beta$ . Further, experiments with USF2 variants mimicking GSK3 $\beta$  phosphorylated USF2 in GSK3 $\beta$ -deficient cells showed that phosphorylation of USF2 by GSK3 $\beta$  did not affect cell proliferation but increased cell migration. Together, this study reports a new mechanism by which USF2 may contribute to cancerogenesis.

**Citation:** Horbach T, Chi TF, Götz C, Sharma S, Juffer AH, et al. (2014) GSK3 $\beta$ -Dependent Phosphorylation Alters DNA Binding, Transactivity and Half-Life of the Transcription Factor USF2. PLoS ONE 9(9): e107914. doi:10.1371/journal.pone.0107914

**Editor:** Yoshiaki Tsuji, North Carolina State University, United States of America

**Received:** June 27, 2014; **Accepted:** August 21, 2014; **Published:** September 19, 2014

**Copyright:** © 2014 Horbach et al. This is an open-access article distributed under the terms of the Creative Commons Attribution License, which permits unrestricted use, distribution, and reproduction in any medium, provided the original author and source are credited.

**Data Availability:** The authors confirm that all data underlying the findings are fully available without restriction. All relevant data are within the paper.

**Funding:** This work was supported by grants from the Wilhelm Sander Foundation (Grant 2008.043.1) to EYD, and from Biocenter Oulu, the Sigrid Juselius Foundation and the Finnish Academy of Science to TK. The funders had no role in study design, data collection and analysis, decision to publish, or preparation of the manuscript.

**Competing Interests:** The authors have declared that no competing interests exist.

\* Email: tkietzm@gwdg.de

## Introduction

The upstream stimulatory factors (USFs) are involved in the transcriptional regulation of various genes whose products contribute to the stress and immune response, to cell cycle and proliferation as well as to lipid and carbohydrate metabolism [1]. In mammals, two different *usf* genes were identified. The *usf1* and *usf2* genes are ubiquitously expressed with varying ratios in different organs [2]. In addition, alternative splicing of the USF2 pre-mRNA gives rise to the generation of USF2a and USF2b [3]. All USF proteins belong to the basic helix-loop-helix leucine zipper (b-HLH-LZ) transcription factor family [4]. They contain a highly conserved USF-specific region (USR) [5] and bind preferably as USF1/USF2 heterodimers [3] to E-boxes with a 5'-CANNTG-3' core sequence in the promoter of their viral or cellular target genes [6].

Generation and observation of USF knockout mice revealed that USF2 seems to be the more important USF variant. While USF1<sup>-/-</sup> mice exhibited a rather normal phenotype, USF2<sup>-/-</sup> mice had a reduced lifespan, decreased fertility and were 20–40% smaller than their wild-type litter mates [7]. Furthermore, USF2 seems to be linked to the development of cancer. While several studies indicated a tumor-suppressive function of USF2 in prostate cancer [8], breast cancer [9] and oral cancer [10], a pro-

liferative function of USF2 was observed in lung cancer cells [11].

Although the above-mentioned studies indicate that USF2 has a crucial role in the organism, especially during cancerogenesis, there is not much knowledge about the mechanisms regulating the activating or suppressive functions of USF2. Eukaryotic cells feature numerous different mechanisms for the regulation of transcription factor function. One versatile option to reversibly regulate the activity of transcription factors is protein phosphorylation. While there is some evidence that USF1 can be phosphorylated by various kinases participating in different signaling pathways [12–20], studies indicating USF2 phosphorylation are rather limited and only one identified PKA as a USF2-phosphorylating kinase [17].

Our own previous work on the role of USF2 on the expression of the cancer marker plasminogen activator inhibitor-1 (PAI-1) [21] suggested that USF2 might be phosphorylated by other kinases than PKA. A kinase which might be of special interest in this regard is glycogen synthase kinase 3 $\beta$  (GSK3 $\beta$ ). This kinase links the PI3K-PKB (AKT) pathway and the Wnt/ $\beta$ -catenin signaling pathway which are both regulating various cellular processes including embryonic development, protein synthesis, cell proliferation, cell differentiation and cell motility [22–24]. GSK3 $\beta$  is an unusual kinase since it is active under resting conditions and

is inhibited both by a PKB (AKT) activating growth factor or a Wnt signal [25]. GSK3 $\beta$  appears to be an attractive candidate kinase for the regulation of USF2 since both proteins seem to be involved in the development of different types of cancer, especially prostate cancer [8,26,27]. In addition, we found that parts of the USF2 protein sequence match with the substrate recognition preferences of GSK3 $\beta$  [28]. Therefore, it was the aim of the present study to analyze the impact of GSK3 on the phosphorylation and function of USF2.

We demonstrate that USF2 can be phosphorylated by GSK3 $\beta$  at two distinct sites. Our data show that these phosphorylation events have the ability to regulate the function of USF2 by altering the DNA binding capacity, the transactivity and the protein stability. Furthermore, we demonstrate that cell migration is influenced by GSK3 $\beta$ -mediated phosphorylation of USF2.

## Materials and Methods

### Materials

All biochemicals and enzymes were of analytical grade and purchased from commercial suppliers. As GSK3 inhibitors, LiCl (Sigma-Aldrich), 6-bromoindirubin-3-oxime (BIO), and 1-Azakenpaullone (both Enzo Life Sciences) were used in the concentrations indicated. BIO and 1-Azakenpaullone were dissolved in DMSO, LiCl in water.

### Plasmid constructs

The expression vector for FLAG-myc-tagged wild-type USF2a (USF2-WT) was generated by PCR using the forward primer 5'-CTGAGAAGCTTATGCTGGACCCGGG-3' and reverse primer 5'-CTGAGTCTAGACTGCCGGGTGCC-3' and a previously described USF2a plasmid [29] as a template. The resulting PCR product was then cloned into the HindIII and XbaI sites of p3xFLAG-myc-CMV24 (Sigma-Aldrich). The forward primer 5'-CAGGGAATTCATGGACATGCTGGAC-3' and the reverse primer 5'-GTATACTCGAGCTGCCGGGTGCC-3' were used to clone a wild-type USF2 product into the EcoRI and XhoI sites of the pGEX-5 $\times$ 1 plasmid (GE Healthcare). The plasmid pcDNA6A-Gal4 containing the Gal4 DNA binding domain was generated by cutting the DNA encoding the Gal4 DNA binding domain from the pSG424 vector [30] and ligating it into the pcDNA6A-Myc-His vector (Life Technologies) via the HindIII and BamHI restriction sites. The plasmid pcDNA6A-Gal4-USF2, allowing expression of a fusion protein of the Gal4 DNA binding domain and the N-terminal part of USF2, was generated by cloning a PCR fragment encoding the N-terminal part of USF2 into the BamHI and XbaI sites of pcDNA6A-Gal4; for the PCR the forward primer 5'-GTATGGTACCTAGGATCCATATGGACATGCTGACCCGGGTCTCGATCCCGCTGCCTC-3' and the reverse primer 5'-CGCGTCTAGAGAATTCCTAGGGTGTCTGGTTCCATC-3' were used. For the generation of deletion and point mutants, the QuikChange Site-Directed Mutagenesis Kit (Agilent Technologies) was used. The expression vectors for pcDNA3-GSK3 $\beta$ -WT, -S9A and -K85A were described before [31,32] and obtained from Addgene (#14753, 14754 and 14755). The pFR-5Gal4-RE-Luc plasmid and the pRL-SV40 plasmid were purchased from commercial suppliers (Agilent Technologies and Promega, respectively) and the luciferase gene constructs containing the promoter regions of human HO-1 from -4000 to +80 [33], of human PAI-1 from -806 to +19 [34] and of rat FAS from -220 to +25 [35] have been described.

### Cell culture, transient transfections and luciferase assays

HeLa and HepG2 cells were maintained in Earle's minimum essential medium (MEM, Sigma-Aldrich); GSK3 $\beta^{+/+}$  and GSK3 $\beta^{-/-}$  mouse embryonic fibroblasts (MEFs), a kind gift from J. Woodgett, were cultured in Dulbeccos modified Eagles medium (DMEM, Sigma-Aldrich). These immortalized MEFs were derived according to approved protocols from GSK3 $\beta$  nullizygous embryos as described [36]. All media were supplemented with 10% fetal bovine serum (FBS, Biochrom), 1% non-essential amino acids and 0.5% ciprofloxacin. The cells were cultured at 37°C in an atmosphere of 16% O<sub>2</sub>, 5% CO<sub>2</sub>, 79% N<sub>2</sub> and 97% humidity. Transient transfections were conducted by the calcium phosphate precipitation method [37] or by using the **Amaya MEF 1 Nucleofector Kit** (VPD-1004, Lonza).

For luciferase assays the transfection efficiency was controlled by cotransfection of a Renilla luciferase expression vector. In brief, one day before transfection 2 $\times$ 10<sup>5</sup> HeLa cells were seeded in 2.5 ml growth medium in 60 mm cell culture dishes. The cells were transfected overnight with 3  $\mu$ g of a Firefly luciferase gene construct, 1  $\mu$ g of expression vector and 50 ng of the Renilla luciferase reporter plasmid (pRL-SV40). The next morning, the medium was replaced by fresh growth medium and the cells were cultured for further 26 h. Then luciferase assays were performed as previously described [38,39].

### RNA preparation and quantitative real-time PCR

Isolation of total RNA was performed using the QiaGen RNeasy Mini Kit (QiaGen, Switzerland) following the manufacturer's instructions. One  $\mu$ g of total RNA was used for first strand cDNA synthesis with the iScript cDNA synthesis Kit (Bio-Rad, Finland). Quantitative real-time PCR was performed in an **Applied Biosystems 7500 Real-Time PCR System** (Life Technologies, Finland) by using an Applied Biosystem Power SYBR green PCR master mix (Life Technologies, Finland). The following primers were used: USF2 forward 5'-GCGTTTCGGCGACCACAATA-3', USF2 reverse 5'-GACTACGCGGTATGTCACCTG-3', FAS forward 5'-GGAGGTGGTGATAGCCGGTAT-3', FAS reverse 5'-TGGGTAATCCATAGAGCCCAG-3', HO-1 forward 5'-GATAGAGCGCAACAAGCAGAA-3', HO-1 reverse 5'-CAGTGAGGCCCATACCAGAAG-3', PAI-1 forward 5'-GTGAATGCCCTCTACTTCAGTG-3', PAI-1 reverse 5'-GCTGCCATCAGACTTGTGGAA-3', ActB forward 5'-ATGCTCCCGGGCTGTAT-3', ActB reverse 5'-CATAGAGTCTCTTGACCCATTC-3', Hprt forward 5'-CGAAGTGTGGATACAGGCC-3', Hprt reverse 5'-GGCAACATCAACAGGACTCC-3'. All primer sets were validated for their product and amplification efficiency using standard dilution analysis and melting curve analysis.  $\beta$ -Actin and Hprt (Hypoxanthine guanine phosphoribosyltransferase) were used as internal controls to normalize the variability in expression levels. The experiments for each data point were carried out in triplicate. The relative quantification of gene expression was determined using the  $\Delta\Delta$ Ct method [40].

### Western blotting, co-immunoprecipitations, protein phosphorylation and half-life studies

Cells were washed with cold PBS and scraped in lysis buffer (50 mM Tris pH 8.0, 5 mM EDTA, 150 mM NaCl, 5 mM DTT, complete mini protease inhibitors (Roche), 25 mM NaF, 1 mM Na<sub>3</sub>VO<sub>4</sub>, 25 mM  $\beta$ -glycerophosphate). The cells were then treated for 20 min in an ice-cooled ultrasonic water bath and subsequently centrifuged at 4°C and 13700 $\times$ g for 20 min. The protein concentration was estimated by the Bradford method.

For the analysis of proteins by Western blotting, cell extracts were denatured with 4x SDS sample buffer (500 mM Tris pH 6.8, 30% glycerol, 10% SDS, 0.01% bromophenol blue, 40 mM DTT) by incubating at 95°C for 10 min. Then the proteins were resolved by 10% SDS-PAGE and blotted to a nitrocellulose membrane. For the analysis of p-USF2, an acrylamide:bisacrylamide ratio of 200:1 was used in the resolving gel.

As primary antibodies monoclonal antibodies against USF2 (6A9; 1:1000; Cat.Nr. H00007392-M03, Abnova), HA-tag (F-7; 1:500; Cat.Nr. sc-7392, Santa Cruz Biotechnology), myc-tag (9B11; 1:1000; Cat.Nr. 2276, Cell Signaling Technology) and  $\alpha$ -tubulin (B-5-1-2; 1:10000; Cat.Nr. T6074, Sigma-Aldrich), as well as polyclonal antibodies against USF2 (N-18; 1:500; Cat.Nr. sc-861, Santa Cruz Biotechnology) were used. Horseradish peroxidase (HRP)-conjugated goat anti-mouse (1:5000, Cat.Nr. 170-6516, Bio-Rad) and goat anti-rabbit IgGs (1:5000; Cat.Nr. 170-6515, Bio-Rad) were used. The enhanced chemiluminescence (ECL) system (GE Healthcare) was used for detection.

For immunoprecipitation experiments, protein samples from HeLa, GSK3 $\beta^{+/+}$ , and GSK3 $\beta^{-/-}$  cells were prepared in lysis buffer (50 mM Tris/HCL, pH 7.5, 150 mM NaCl, 1% Triton X-100, 2 mM EDTA, 2 mM EGTA, 1 mM PMSF and complete protease inhibitor cocktail tablet (Roche)). After scraping, lysates were incubated with continuous shaking at 4°C for 20 min and then they were centrifuged at 12,000 g at 4°C for 15 min [41]. To recover USF2 immunoprecipitates, 250  $\mu$ g of total protein was incubated with 2  $\mu$ g antibody for 1 h at 4°C before Sepharose beads (30  $\mu$ l per reaction mixture) were added for 12 h. Thereafter, the beads were washed five times with lysis buffer and recovered, pellets were dissolved in 2 X Laemmli buffer, loaded onto a SDS-PAGE gel, blotted and detected with antibodies against phospho-serine and phospho-threonine, respectively.

For dephosphorylation experiments, cell extract (90  $\mu$ g protein) was incubated with 40 u calf intestinal phosphatase (CIP, Fimnzymes) at 37°C for 5 min. In the appropriate control sample the enzyme was replaced by water.

In half-life studies, GSK3 $\beta^{+/+}$ , and GSK3 $\beta^{-/-}$  cells were treated with 10  $\mu$ g/ml cycloheximide (CHX, Sigma- Aldrich) for the indicated time periods. Whole cell extracts were prepared as above and 100  $\mu$ g of protein was loaded onto 10% SDS-polyacrylamide gel. After electrophoresis and electroblotting onto a nitrocellulose membrane, proteins were detected with antibodies against USF2 and quantified with Fiji (NCBI) software.

### Phosphoprotein staining

Immunoprecipitated proteins (250  $\mu$ g endogenous proteins or 150  $\mu$ g overexpressed proteins) were denatured and subjected to 10% SDS-PAGE. Phosphoproteins were stained with Pro-Q Diamond Phosphoprotein Stain (Life Technologies) and detected with a wavelength of 532 nm using the Typhoon 9400 (GE Healthcare). Subsequently, total proteins were detected by silver staining [42].

### Expression and purification of proteins, radioactive kinase assays

Using the pGEX-5 $\times$ 1 system (GE Healthcare), GST fusion proteins were expressed in *E. coli* BL21 (DE3) at 30°C and purified with Glutathione Sepharose beads as described previously [43]. Purified GST fusion proteins (1.5  $\mu$ g) or proteins immunoprecipitated from whole cell extracts (350  $\mu$ g) were incubated in kinase assay buffer (15 mM MOPS pH 7.2, 15 mM MgCl<sub>2</sub>, 3 mM EGTA, 1.2 mM EDTA, 150  $\mu$ M DTT, 6 mM  $\beta$ -

glycerophosphate) containing 20 ng of active, recombinant full-length human GSK3 $\beta$  (SignalChem), 50  $\mu$ M unlabeled ATP and 1.5  $\mu$ Ci [ $\gamma$ -<sup>32</sup>P] ATP at 30°C for 20 min. The proteins were denatured by incubating with 4x SDS sample buffer at 95°C for 10 min. Following separation of the proteins by 10% SDS-PAGE, the gel was exposed to a Kodak phosphor imaging screen overnight and thereafter autoradiography was detected with a Molecular Imager FX using the Quantity One software (all BIO-RAD). Afterwards, the total proteins were detected by Coomassie staining or silver staining.

### Chromatin immunoprecipitation (ChIP)

Wild-type (WT) and GSK3 $\beta^{-/-}$  MEFs were seeded in 15 cm cell culture dishes and ChIP was performed as described previously [44]. In brief, after cross-linking, cell lysis and sonication, chromatin samples were incubated with anti-USF2 antibody (N-18, Cat.Nr. sc-861, Santa Cruz Biotechnology), anti-RNA polymerase II antibody (N-20, Cat.Nr. sc-899X, Santa Cruz Biotechnology) or IgG preimmune serum (BioScience) in an ultrasonicator bath for 1 h at 4°C; after centrifugation, the precleared samples were mixed with protein G Sepharose beads for 1 h at 4°C. After several washes, Chelex 100 (Bio-Rad) suspension was added to the beads and the samples were boiled for 10 min; after cooling down to RT, Proteinase K was added and the samples were incubated for 30 min at 55°C with shaking, boiled again for 10 min and centrifuged [44]. The isolated DNA was subjected to quantitative PCR that was performed with the 7500 Real-Time PCR System (Applied Biosystems) using the Power SYBR Green Master Mix (Life Technologies). The ChIP primers used were: PAI-1 forward, 5'-GTCTAGACGACCGAC-CAGCCAAA-3', PAI-1 reverse, 5'-GAAATGTCTGGGCTGCCCGC-3'. HO-1 forward, 5'-GCCTCCGGGCTGGATGTTG-3' and HO-1 reverse, 5'-GGAGACCGTGAGCGAGCAGC-3', FAS forward, 5'-GACGCTCATTGGCCTGGGC-3' and FAS reverse, 5'-ACGCCGCTGCCGTCTCTCT-3'. As a positive control, a RNA polymerase II antibody was used to immunoprecipitate RNA polymerase II from an actively expressed housekeeping gene promoter; the mouse  $\beta$ -actin promoter was amplified with the following forward 5'-GTGAGTGAGCGACGCGGAGCCAA-3', and reverse 5'-CTTACCTGGTGGCGGGTGTGGA-3' primers [45]. All primer sets were validated for their product and amplification efficiency using standard dilution analysis and melting curve analysis. Differences in the USF2 and RNA Polymerase II DNA binding efficiency in wild-type (WT) and GSK3 $\beta^{-/-}$  MEFs were calculated by the percent input method using the formula  $\text{Ct}_{100} \times 2^{-(\text{Adjusted input} - \text{Ct}(\text{IP}))}$ , where input adjustment is calculated using the formula  $\text{raw Ct}/(\text{Ct Input} \times \log_2 \text{ of the dilution factor})$  (dilution factor (DF) is equal to 1/fraction input).

### Proliferation and cell migration assay

For BrdU, MTT and cell migration assays GSK3 $\beta^{-/-}$  MEF cells were seeded onto 10 cm cell culture dishes and one day later the cells were transfected by using the **Amara MEF 1 Nucleofactor** Kit (VPD-1004, Lonza) with 5  $\mu$ g of expression vectors for USF2-S155A/T230A, USF2-S155D/T230D or an empty vector. After 20 h,  $4 \times 10^4$  electroporated cells were seeded in 500  $\mu$ l growth medium into a 24-well culture dish for the MTT assay,  $1 \times 10^4$  electroporated cells were seeded in 100  $\mu$ l growth medium into a 96 well culture dish for the BrdU assay and  $1 \times 10^4$  electroporated cells were seeded for migration assay (see below). From another aliquot of the electroporated MEFs whole cell extracts were prepared for the control of transfection efficiency by

Western blotting. Cells plated for the MTT assay and the BrdU assay were cultured for further 30 h. For the MTT assay cells were stained with 50  $\mu$ l MTT solution (4 mg/ml in PBS) for 1.5 h and the absorbance was measured at a wavelength of 570 nm. The BrdU assay (Calbiochem) was performed according to the manufacturer's instructions and the absorbance was measured at dual wavelengths of 450–540 nm.

Cell migration was measured by using medium-treated 24-well Transwell chambers (BD Bioscience) with 8.0  $\mu$ m polycarbonate membranes. The bottom chamber was filled with 600  $\mu$ l medium containing 10% fetal calf serum; cells were seeded into the top chamber at a density of  $1 \times 10^4$  cells per well in 100  $\mu$ l serum-free medium. After incubation in a humidified incubator with 5% CO<sub>2</sub> at 37°C for 4 h, cells were fixed with 4% paraformaldehyde and the non-migratory cells were scraped off from the top of the Transwell with a cotton swab. The migrated cells attached to the bottom chamber were stained with 0.0075% crystal violet. Crystal violet absorption at 595 nm was measured in a Tecan Infinite M1000Pro microplate reader. For each migratory condition, two identical replicates were performed.

### In silico analysis of phosphorylated USF2 structures

A homology model of USF2 was built using the I-TASSER online software [46,47], followed by an energy minimization of the predicted structure. The energy minimization and subsequent computer simulations were all completed with Gromacs 4.0.7. [48] and GROMOS96 43a1 force field [49]. The residues S155 or T230 were phosphorylated employing the molefacture plugin in VMD [50].

The resulting structures (native, S155 phosphorylated, T230 phosphorylated) were each solvated in a rectangular box containing SPC waters [51], under periodic boundary conditions. After a steepest-descent energy minimization of each system until they converged to 10 kJ mol<sup>-1</sup> nm<sup>-1</sup>, a short 100 ps in the NVT (constant number of atoms, constant volume, constant temperature) ensemble was carried to equilibrate the given system. This was followed by a 15 ns production run in the NPT (constant number of atoms, constant pressure, constant temperature) ensemble. All simulations were carried out at 1.0 atm constant pressure using the Parrinello-Rahman barostat [52] and at 300 K constant temperature using V-rescale algorithm [53] with coupling constants of 0.5 and 0.1 ps, respectively. The time step used for the simulations was 2 fs. A cut-off of 12 Å was employed for the short-range non-bonded interactions. Long-range electrostatic interactions were computed using the particle mesh Ewald (PME) method [54]. All bonds were constrained employing the LINCS algorithm [52]. Water molecules were constrained using the SETTLE algorithm [55].

### Statistical analysis

Each experiment was performed at least three times and representative data are shown. Data in bar graphs are given as mean values  $\pm$  standard deviation (SD). Statistical differences were calculated by using the Student t-test with error probabilities of  $p < 0.05$  to be significant.

### Ethics statement

All experimental procedures involving animal-derived cell lines were approved and performed only under permissions from the Animal Experiment Board of Finland following the regulations of the EU Directive 86/609/EEC, the European Convention ETS123 and the national legislation of Finland.

## Results

### GSK3 $\beta$ phosphorylates USF2

GSK3 has been found to phosphorylate many proteins among them transcription factors playing important roles in a variety of cellular processes [56]. Since we found that parts of the USF2 protein sequence match with the substrate recognition preferences of GSK3 $\beta$  [28] we aimed to investigate whether GSK3 $\beta$  can phosphorylate USF2 in intact cells and whether this affects USF2 function. To do this, we first immunoprecipitated USF2 from GSK3 $\beta$ -deficient mouse embryonic fibroblasts (GSK3 $\beta$ <sup>-/-</sup> MEFs) and their wild-type counterparts (GSK3 $\beta$ <sup>+/+</sup> MEFs) and visualized threonine and serine phosphorylated USF2 via immunodetection with phospho-threonine and phospho-serine antibodies. We found that threonine and serine phosphorylated USF2 could be detected in the wild-type cells whereas none of these forms could be detected in GSK3 $\beta$ <sup>-/-</sup> MEFs (Fig. 1A). Next, we immunoprecipitated USF2 from HeLa cells transfected with a GSK3 $\beta$  expression vector and subsequently determined the phosphorylation of USF2 by phosphoprotein staining. We observed a positive phosphostaining in untreated HeLa cells indicating that some USF2 already exists in its phosphorylated form. In addition, a higher molecular weight and consequently slower migrating band indicating hyperphosphorylated USF2 could be detected upon overexpression of GSK3 $\beta$  (Fig. 1B).

We then used the molecular weight shift of phosphorylated USF2 to analyze phosphorylation of USF2 by Western blotting upon treatment of cells with 3 different kinase inhibitors supposed to be selective for GSK3 $\beta$ . All three kinase inhibitors, namely BIO, LiCl and 1-Azakenpaullone, prevented the appearance of phospho-USF2 (Fig. 1C). To further confirm that the band of higher molecular weight appearing after overexpression of GSK3 $\beta$  corresponds to phosphorylated USF2, cell extracts were incubated with calf intestinal phosphatase (CIP). After dephosphorylation with CIP, the band with the higher molecular weight disappeared, confirming that it indeed corresponds to the phospho-USF2 (Fig. 1D).

In addition to the experiments in HeLa cells, we were able to show that GSK3 $\beta$ -dependent phosphorylation of USF2 also occurs in HepG2 cells and in the human prostate cancer cell lines LNCaP and PC-3 (data not shown). Together, these data, in particular the data obtained from the GSK3 $\beta$ <sup>-/-</sup> MEFs indicate that GSK3 $\beta$  phosphorylates USF2 in cells.

### Mapping of the GSK3 $\beta$ phosphorylation sites within USF2

To further investigate the details of GSK3 $\beta$ -dependent USF2 phosphorylation, we aimed to map the exact phosphorylation sites within USF2 by means of radioactive kinase assays with recombinant GST tagged USF2 proteins *in vitro*. In addition to full length USF2, we also purified 6 different deletion variants (Fig. 2A) to identify the domain within USF2 that can be phosphorylated by GSK3. In line with the previous data from the cells, we could confirm that GSK3 phosphorylates wild-type USF2 (Fig. 2B).

Next, we tested the 6 USF2 deletion mutants in kinase assays to determine which domains of USF2 can be phosphorylated by GSK3 $\beta$  (Fig. 2C). We detected a strong phosphorylation of the protein containing the USR (200–231) while a weaker phosphorylation occurred with the protein containing the N-terminal domain up to amino acid 161. No phosphorylation could be observed with the proteins containing the amino acids 157–199 or the b-HLH-LZ domain (232–346).

Based on these results we then aimed to identify the exact phosphorylation sites within these USF2 proteins. To do this, we



**Figure 1. USF2 is phosphorylated by GSK3 $\beta$ .** (A) USF2 was immunoprecipitated from GSK3 $\beta^{+/+}$  and GSK3 $\beta^{-/-}$  cells and phospho-USF2 protein levels were detected with phospho-threonine or phospho-serine antibodies. (B) USF2 was immunoprecipitated from HeLa cells transfected with pcDNA3-GSK3 $\beta$ -WT-HA. Following SDS-PAGE phosphoproteins were visualized with the Pro-Q Diamond Phosphoprotein Gel Stain. The total protein amount was detected by silver staining and GSK3 $\beta$  expression was verified by Western blotting. (C) Where indicated, HeLa cells transfected as above were treated with the GSK3 selective inhibitors BIO (1  $\mu$ M), LiCl (10 mM), 1-Azakenpaulone (Aza, 7.5  $\mu$ M) for 1 h. Proteins were isolated 24 h after transfection and detected by Western blotting. (D) Cells were transfected with expression vectors for USF2 and GSK3 $\beta$  and the cell extract was incubated with calf intestinal phosphatase (CIP) or only with buffer (Mock). Proteins were detected by Western blotting. doi:10.1371/journal.pone.0107914.g001

first mutated all 8 phosphorylatable serine and threonine residues within the USR (200–231) separately and converted them into non-phosphorylatable alanine residues. Since the amino acids 218–222 (THPYS) within the USR perfectly match the GSK3 $\beta$  minimal recognition motif S/T-X-X-X-pS/pT, where the N-terminal S/T is the proper GSK3 $\beta$  phosphorylation site and the C-terminal S/T is the site of priming phosphorylation, we also generated a T218A/S222A double mutant. The kinase assays with these USR mutants and GSK3 $\beta$  revealed that T230 is the proper phosphorylation site within this domain, since replacement of this residue by alanine completely abolished the phosphorylation. All other USR single point mutants and the T218A/S222A double mutant were still phosphorylatable by GSK3 $\beta$  (Fig. 2D).

The N-terminal domain of USF2 comprising the amino acids 1–161 contains 18 phosphorylatable serine and threonine residues. We screened this sequence for minimal GSK3 $\beta$  recognition motifs and found one of these motifs within this N-terminal domain. Based on this, S151 would be the proper GSK3 phosphorylation site and S155 would be the site of priming phosphorylation. Hence, both sites were replaced by alanine. Additionally, S155 was substituted by aspartate; also a S151A/S155D double mutant was constructed. Kinase assays with these proteins revealed that any modification of S155 totally abolished GSK3 $\beta$ -mediated incorporation of radioactivity whereas the S151A mutant was still phosphorylatable. Since mutation of S155 completely prevented GSK3 $\beta$ -mediated phosphorylation, we concluded that this residue is the exclusive GSK3 $\beta$  site in this N-terminal domain of USF2 (Fig. 2E).

To verify the importance of S155 and T230 within full length USF2, we performed a kinase assay with recombinant GSK3 $\beta$  and full-length wild type USF2 or the respective S155 and T230 mutants which we expressed and immunoprecipitated from HeLa cells. The USF2-WT protein and the single mutants USF2-S155A, USF2-T230A, and as a control USF2-T228A were phosphorylatable by GSK3 $\beta$ . By contrast, when both S155 and T230 were substituted with alanine (S155A/T230A) phosphorylation by GSK3 $\beta$  was completely prevented (Fig. 2F).

Together, these data show that there are two residues within USF2, namely S155 and T230, which can be phosphorylated by GSK3 $\beta$ .

### Phosphorylation enhances the transactivity of USF2

To test whether the identified phosphorylation sites are crucial for the transactivity of USF2 we performed luciferase assays. We took advantage of the Gal4 system to assess the impact of the detected phosphorylation sites on the USF2 transactivity independent from their effect on the DNA binding capacity. Therefore, we generated constructs in which the USF2 DNA binding b-HLH-LZ domain (aa 232–346) was replaced with the DNA binding domain

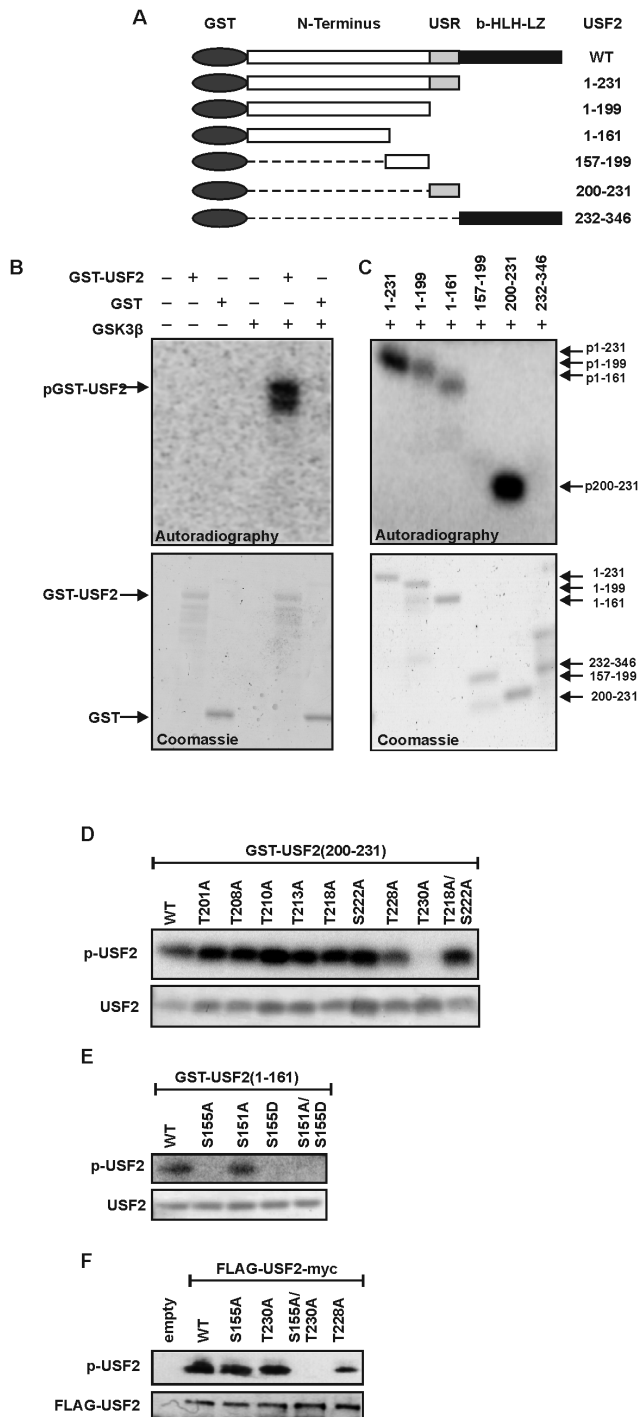


**Figure 2. GSK3 $\beta$ -mediated phosphorylation occurs in two USF2 domains.** (A) Schematic representation of the USF2 deletion mutants used to identify the domains that are phosphorylated by GSK3 $\beta$ . (B–E) Purified GST-tagged USF2 proteins were incubated with recombinant human GSK3 $\beta$  in the presence of [ $\gamma$ - $^{32}$ P] ATP. Proteins were separated by SDS-PAGE and incorporated radioactivity was detected by autoradiography. The total amount of proteins was detected by Coomassie staining. (F) HeLa cells were transfected with expression vectors for USF2 or the empty vector. USF2 was immunoprecipitated from the total cell extract and then incubated with recombinant human GSK3 $\beta$  in the presence of [ $\gamma$ - $^{32}$ P] ATP. Proteins were separated by SDS-PAGE and incorporated radioactivity was detected by autoradiography. The total amount of proteins was detected by silver staining.  
doi:10.1371/journal.pone.0107914.g002

of the transcription factor Gal4. In addition to the resulting construct encoding the wild type Gal4-USF2 fusion protein (Gal4-USF2(1-231)-WT), another plasmid encoding a fusion protein in which the two GSK3 $\beta$  phosphorylation sites were substituted with alanine (Gal4-USF2(1-231)-S155A/T230A) was generated. As a control constructs encoding only the Gal4 DNA binding domain were used. These Gal4 fusion constructs were then cotransfected with a plasmid containing the luciferase gene under the control of 5 Gal4 response elements (RE). Thus, changes in the measured luciferase activity reflect the transactivity of the transcription factor USF2. While the presence of the constitutively active GSK3 $\beta$ -S9A significantly increased the observed luciferase activity with the Gal4-USF2(1-231)-WT construct, no change in luciferase activity could be detected with the Gal4-USF2(1-231)-S155A/T230A double mutant (Fig. 3A). Western Blot controls revealed that all Gal4-USF2 proteins used in the luciferase experiments were correctly expressed and their levels were not affected by overexpression of GSK3 $\beta$  (Fig. 3B). Together, these data strongly suggest that phosphorylation of USF2 by GSK3 $\beta$  is critical for the regulation of USF2 transactivity.

### Phosphorylation of USF2 increases expression of its target genes

Next, we wanted to know whether the phosphorylation of USF2 affects expression of the USF2 target genes heme oxygenase 1 (HO-1), plasminogen activator inhibitor 1 (PAI-1), and fatty acid synthase (FAS). To test this, we used GSK3 $\beta^{+/+}$  and GSK3 $\beta^{-/-}$  cells and measured FAS, HO-1, and PAI-1 mRNA and protein levels. Indeed, FAS, HO-1, and PAI-1 mRNA levels (Fig. 3C) as well as protein levels (Fig. 3D) were reduced significantly in the GSK3 $\beta^{-/-}$  cells. By contrast, non-USF2 targets but GSK3 $\beta$  regulated proteins like  $\beta$ -catenin and c-Myc were upregulated in GSK3 $\beta^{-/-}$  cells (Fig. 3D). Thus, these data indicate that phosphorylation of USF2 by GSK3 $\beta$  enhances expression of USF2 target genes.

### Phosphorylation of USF2 increases its DNA binding to target gene promoters

Since S155 and T230 are close to the DNA binding domain of USF2, we also decided to investigate whether the phosphorylation by GSK3 $\beta$  affects binding of USF2 to its target DNA. To do this, we used again GSK3 $\beta^{+/+}$  and GSK3 $\beta^{-/-}$  cells and performed chromatin immunoprecipitations with an USF2 antibody followed by quantitative PCR with primers encompassing the USF binding sites within the FAS, HO-1, and PAI-1 promoter [21]. The chromatin immunoprecipitation studies show that USF2 strongly binds to the FAS, HO-1, and PAI-1 promoters in GSK3 $\beta^{+/+}$  cells. By contrast, binding of USF2 to the FAS promoter was almost lost in GSK3 $\beta^{-/-}$  cells and binding to the HO-1 and PAI-1 promoter was reduced by 60% and 70%, respectively (Fig. 3E). Furthermore, binding of RNA polymerase II to the  $\beta$ -actin promoter, used as a positive control, showed no significant difference between WT- and GSK3 $\beta^{-/-}$  cell lines (Fig. 3E). Together, these data indicate that phosphorylation of USF2 by GSK3 $\beta$  contributes to the regulation of its DNA binding capacity.

To address whether the reduced DNA binding and transactivation capacity has direct transcriptional consequences, we used FAS, HO-1, and PAI-1 promoter luciferase constructs and cotransfected them with vectors for wild-type USF2 (USF2-WT), USF2-S155A, USF2-T230A or the S155A/T230A double mutant. As a control, the promoter luciferase constructs were cotransfected with a USF2 plasmid in which T228 was substituted with alanine (Fig. 4). The luciferase assays revealed that wild-type

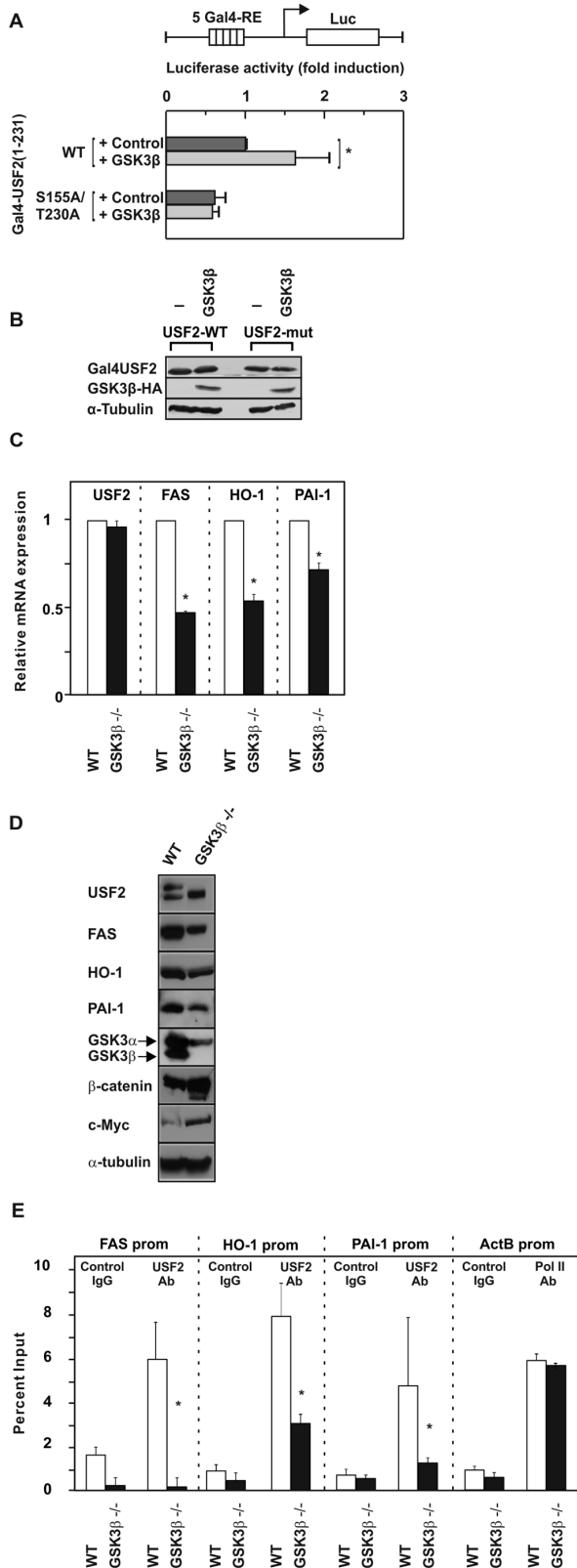


**Figure 3. GSK3 $\beta$ -mediated phosphorylation of USF2 affects its transactivity, DNA binding and target gene expression.** (A) HeLa cells were cotransfected with pFR-5Gal4-RE-Luc, an expression vector for constitutively active GSK3 $\beta$ -S9A and WT or mutant pcDNA6-Gal4-USF2 (1-231) or the appropriate empty Gal4 vector. The luciferase activity was calculated as fold induction compared to the Gal4-USF2 (1-

231)-WT luciferase activity after subtracting the values from the empty Gal4 expression vector. \*, significant differences control vs. GSK3 $\beta$ . (B) Representative Western blot of the transfected constructs. 50  $\mu$ g of protein from transfected cells were probed with an antibody against Gal4, HA-tag and  $\alpha$ -tubulin. (C) Quantitative RT-PCR analyses of FAS, HO-1, PAI-1 and USF2 mRNA levels in GSK3 $\beta$ <sup>+/+</sup> and GSK3 $\beta$ <sup>-/-</sup> cells. \*, significant differences WT vs. GSK3 $\beta$ <sup>-/-</sup>. (D) Western Blot analyses of FAS, HO-1 and PAI-1 expression in GSK3 $\beta$ <sup>+/+</sup> and GSK3 $\beta$ <sup>-/-</sup> cells. 50  $\mu$ g of protein were subjected to Western analysis with antibodies against FAS, HO-1, PAI-1 or  $\beta$ -catenin, c-Myc or  $\alpha$ -tubulin; the latter served as a loading control. (E) ChIP was performed in GSK3 $\beta$ <sup>+/+</sup> and GSK3 $\beta$ <sup>-/-</sup> cells with either USF2 antibody, control IgG or RNA Pol II antibody. The quantitative PCR was performed with primers amplifying the FAS, HO-1, and PAI-1 promoter containing the USF2 binding sites, and with primers amplifying the  $\beta$ -actin promoter binding RNA Pol II as outlined in Materials and Methods. \*, significant differences WT vs. GSK3 $\beta$ <sup>-/-</sup>. doi:10.1371/journal.pone.0107914.g003

USF2 induced luciferase activity significantly with all tested promoters. By contrast, the USF2-S155A and USF2-T230A single mutants and the USF2-S155A/T230A double mutant diminished luciferase activity compared to USF2-WT with all tested promoter constructs. The control mutant USF2-T228A induced luciferase activities like USF2-WT (Fig. 4). Together, these data indicate that phosphorylation of USF2 by GSK3 $\beta$  at S155 and T230 are important for the regulation of USF2 DNA binding and transactivity.

### Phosphorylation changes the 3-dimensional structure of USF2

Next we aimed to understand whether the phosphorylation of USF2 at S155 or T230 affects the 3-dimensional structure of the protein. Since there is no crystal structure for full length USF2 available we performed a series of molecular dynamics simulations of USF2 when S155 and T230 remained non-phosphorylated (native protein) and when S155 and T230 were phosphorylated. The modeled molecular structure of the native non-phosphorylated USF2 protein indicated that the protein is composed of two domains (Fig. 5A). The two GSK3 $\beta$  phosphorylation sites S155 and T230 are located at the interface of the two domains. The respective 15 ns molecular dynamics simulations with phospho-S155 and phospho-T230 were sufficient long for a proper stabilization of the C-alpha root mean square deviations (data not shown). We found that the distance between the two domains increased (Fig. 5B–D) in phosphorylated USF2. In particular, the distance between side chain oxygen atoms of S155 and T230 residues were increased by 10  $\text{Å}$  (Fig. 5). Together, the results show that phosphorylation of USF2 by GSK3 $\beta$  at S155 and T230 effectively increases the separation of the two major USF2 domains suggesting that this contributes to the changed DNA binding and transactivity.

### GSK3 $\beta$ - affects the half-life of USF2

Often phosphorylation or dephosphorylation changes the stability of a protein. Hence, we investigated whether GSK3 $\beta$ -dependent phosphorylation affects USF2 protein stability. Therefore, GSK3 $\beta$ <sup>+/+</sup> and GSK3 $\beta$ <sup>-/-</sup> cells were treated with the protein synthesis inhibitor CHX and the level of endogenous USF2 was monitored by Western blotting. While the USF2 half-life in the control cells was about 38 h, the half-life in cells lacking GSK3 $\beta$  was estimated to be about 31 h (Fig. 6). These data show that GSK3 $\beta$ -mediated phosphorylation increases the protein stability of USF2.

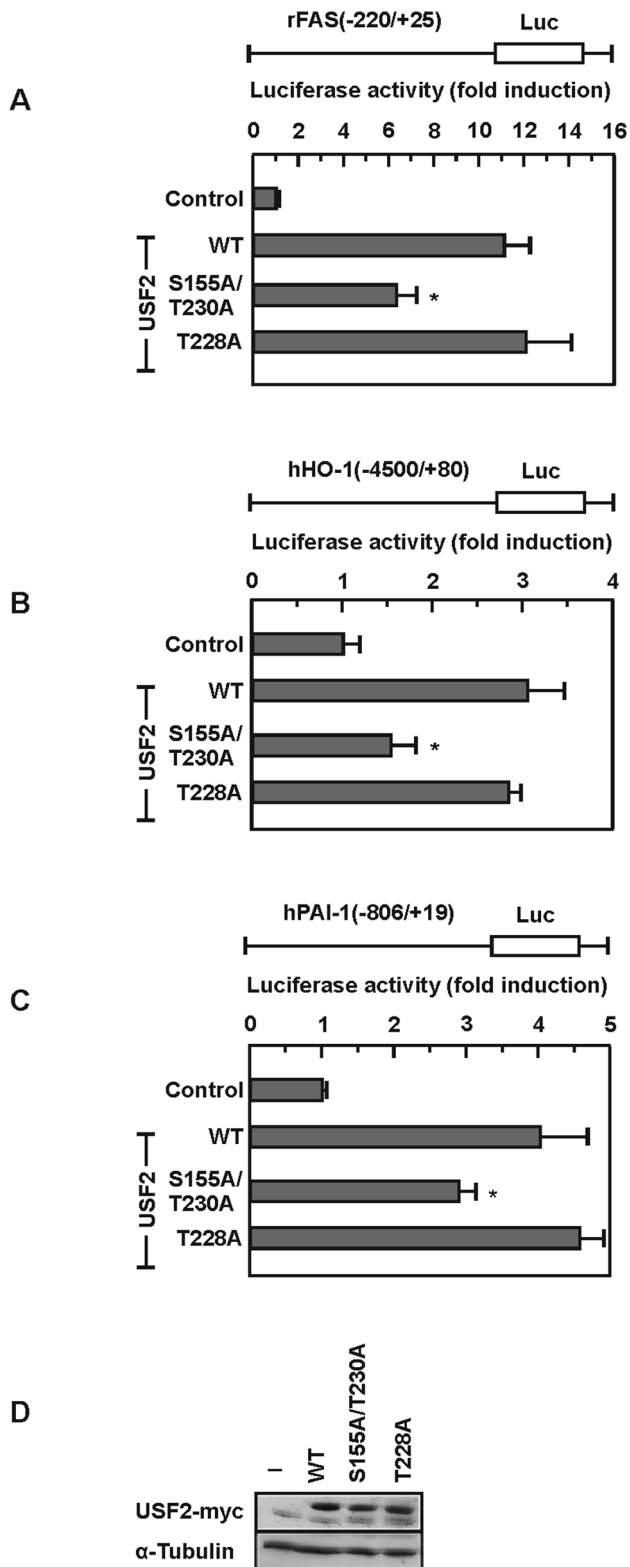


**Figure 4. GSK3 $\beta$ -mediated phosphorylation of USF2 affects activation of target gene promoters.** (A–C) HeLa cells were cotransfected with the indicated luciferase gene construct and with WT or mutant p3xFLAG-USF2-myc-CMV24 or the appropriate empty vector. The measured luciferase activity is plotted as fold induction compared to the luciferase activity measured in the control transfected with the empty expression vector. \*, significant difference WT vs. mutant. (D) Representative Western blot of the transfected constructs.

50  $\mu$ g of protein from transfected cells were probed with an antibody against myc-tag and  $\alpha$ -tubulin.  
doi:10.1371/journal.pone.0107914.g004

### The phosphorylation of USF2 by GSK3 $\beta$ does not affect cell proliferation but influences cell migration

We next determined whether the GSK3 $\beta$  mediated USF2 regulation is involved in cell proliferation. To test this, we used GSK3 $\beta$ <sup>-/-</sup> cells and transfected them with the non-phosphorylatable USF2 variant S155A/T230A or the USF2 variant S155D/T230D mimicking a GSK3 phosphorylated status and measured the overall cellular viability and metabolic activity of the cells in an MTT assay as well as bromodesoxyuridine (BrdU) incorporation into newly synthesized DNA. We found that none of the USF2 variants exerted an effect on cellular viability and DNA synthesis (Fig. 7A).

We also analyzed cellular viability and BrdU incorporation in HeLa cells expressing the non-phosphorylatable USF2 -S155A/T230A or the USF2 variant S155D/T230D mimicking a GSK3 phosphorylated status along with GSK3 $\beta$ . Again, it turned out that neither the non-phosphorylatable variant USF2-S155A/T230A nor the phospho mimicking USF2 variant S155D/T230D had an effect on cellular viability or BrdU incorporation (data not shown). These data suggest that phosphorylation of USF2 by GSK3 $\beta$  has no impact on overall cellular viability and proliferation.

To analyze whether the GSK3 $\beta$ -mediated effects on USF2 have an impact on the invasive cellular potential, we performed transwell migration assays with GSK3 $\beta$ <sup>-/-</sup> cells and GSK3 $\beta$ <sup>-/-</sup> cells transfected with either the non-phosphorylatable USF2 variant S155A/T230A or the phospho-mimicking variant S155D/T230D. A significant increase in migration could be detected with GSK3 $\beta$ <sup>-/-</sup> cells expressing the phospho-mimicking variant S155D/T230D; which reflects GSK3 phosphorylated USF2 whereas the USF2 S155A/T230A variant slightly decreased migration (Fig. 7B, C, D). Together, these data show that lack of GSK3 $\beta$  can reduce invasive cellular growth in a USF2-dependent manner.

### Discussion

In the current study we investigated the impact of GSK3 $\beta$  on the phosphorylation and function of the transcription factor USF2. Our data demonstrated several new findings with respect to USF2 phosphorylation and regulation. First, it was found that GSK3 $\beta$  phosphorylates USF2 at S155 and T230. Second, phosphorylation of USF2 at S155 and T230 increased its DNA binding, transactivity, half-live, and target gene expression. Third, phosphorylation of USF2 by GSK3 $\beta$  did not affect cell proliferation but increased cell migration.

From the two USFs known, mainly USF2 appeared to have a direct link to cell migration and thus to cancerogenesis. This was first highlighted by a study investigating hormone refractory prostate cancer samples. Half of the hormone refractory prostate cancer samples displayed a loss of chromosome 19q ter-q13.1 [57] which includes the region with the *usf2* gene [58]. A reintroduction of an intact human chromosome 19 into a tumorigenic prostate cell line reduced tumorigenicity in athymic nude mice [59]. In addition, USF2 was found to be affected in breast [9], lung [11], oral [10] and colorectal [60] cancer suggesting a more general role of USF2 in tumorigenesis. This suggestion is supported by reports showing that USF2 also regulates the expression of the APC, BRCA2 and p53 tumor suppressor genes [61–63] and our previous studies showing that USF2 plays an important role in regulating the expression of the cancer marker PAI-1 [21,64].



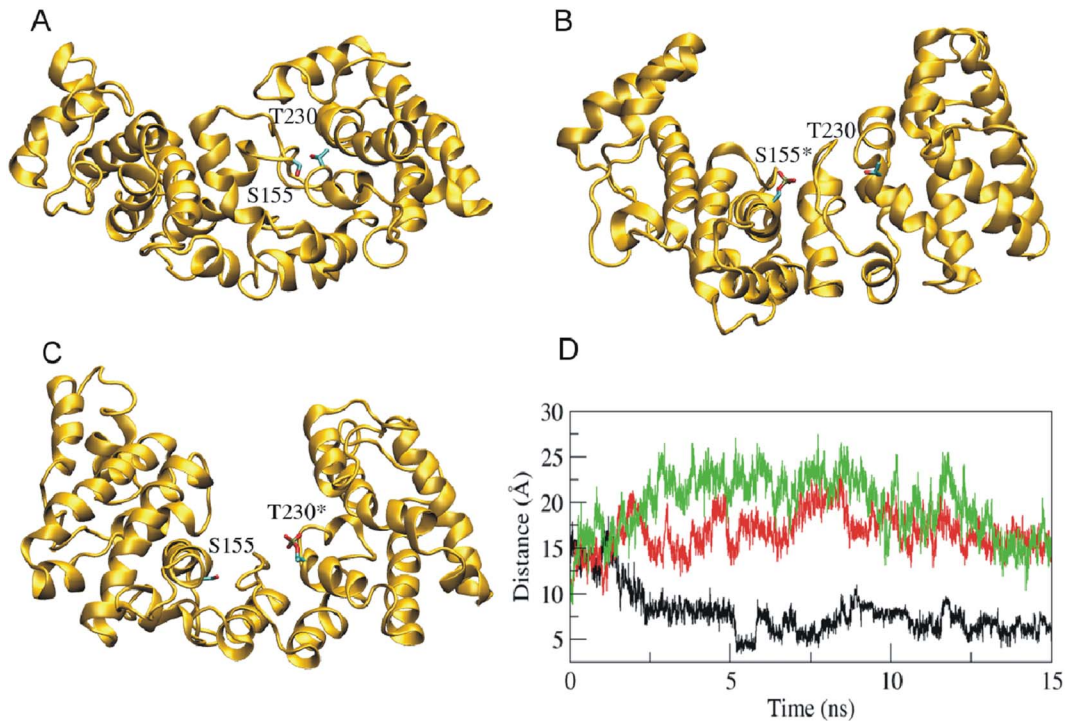


**Figure 5. Phosphorylation of USF2 by GSK3 $\beta$  increases domain (residue) distance.** (A–C) Simulated structures of wild type (A), S155 phosphorylated (B), and T230 phosphorylated (C) USF2 from the MD simulation trajectories. The side chains of Ser155 and Thr230 are shown in stick representation. Phosphorylated amino acids are labeled with an asterisk (\*). The distance between side chain oxygen of S155 and T230 were analyzed (D). Phosphorylation of S155 (red) or T230 (green) increases the distance compared to non-phosphorylated USF-2 (black). doi:10.1371/journal.pone.0107914.g005

Although these observations suggest that USF2 plays an important role during cancerogenesis, it was almost unknown which mechanisms are responsible for the regulation of the transcription factor. The current study narrows this gap and is the first to report that phosphorylation of USF2 by GSK3 $\beta$  affects DNA binding, transactivation and protein half-life. These data are in line with previous reports from other groups and our own work indicating that the effect of USF2 on cancerogenesis may be due to post-translational modifications like phosphorylation. Although no mechanism was determined, some reports indicated that the USF-specific region (USR) appears to be crucial for the function of USF since the simple use of USF2 variants consisting just of the leucine zipper (LZ), basic helix-loop-helix (bHLH) and basic region (BR) which are involved in dimerization, DNA binding and nuclear localization [65] or the N-terminally located transactivation domain (TAD) had no important effect on colony formation [66] or PAI-1 expression [21,64].

Interestingly, when inspecting the USF2 sequence for the presence of GSK3 sites, we found the existence of some S/T-X-X-X-S/T motifs, which are typical recognition motifs for GSK3 $\beta$ . Although not strictly required, priming phosphorylation seems to increase substrate phosphorylation by GSK3 $\beta$  [18]. Within the minimal GSK3 recognition motif, the first S/T is the proper GSK3 $\beta$  target site, X is any amino acid and the C-terminal S/T residue is the site of priming phosphorylation [28]. The USR sequence 218-THPYS-222 completely matches this consensus sequence. However, the kinase assays and transfection experiments with USF2 variants mutated at the putative GSK3 sites T218 and S222 did not show that these residues are real GSK3 sites. Instead, T230 was determined to be the site of USR phosphorylation. Similarly, analyzing the USF2 motif 151-SNGGS-155, we found that instead of the theoretical phosphor-

ylation site S151 the real site of GSK3 $\beta$ -dependent phosphorylation is S155. A recent study on the USF1 protein which is a product from a different gene but can heterodimerize with USF2 identified Thr153 and S186 to be GSK3 sites [18]. Although some similarities between USF1 and USF2 exist, they appear to have different functions, and different target genes which is also substantiated by significantly different phenotypes of USF1 and USF2 knockout mice. Moreover, like in the present study there is also no priming phosphorylation at the amino acid in +4 position of USF1 S186 [18]. These findings are conform to other studies in which for example the transcription factors c-Jun [67], p53 [68] and c-Myb [69] were found to be phosphorylated by GSK3 $\beta$  at sites not matching the minimal recognition motif. Checking the USF2 sequence adjacent to the two identified phosphorylation sites S155 and T230 more closely revealed that the n+4 position, which is the site of priming phosphorylation in the preferred GSK3 $\beta$  recognition motif, is a glutamate (E) residue in both cases (155-SPAAE, 230-TPRDE). Considering that glutamate has a negative charge like a phosphate group, it is possible that the glutamate residue can mimic priming phosphorylation and thereby favors GSK3 $\beta$ -mediated phosphorylation of the two identified USF2 sites.

In addition to our own experiments, the only data for USF2 phosphorylation so far came from a study of the bovine system investigating the effect of forskolin and protein kinase A (PKA) on the prostaglandin G/H-2 synthase promoter. That study showed that USF2 contains three PKA phosphorylation sites and that overexpression of PKA enhanced USF DNA binding in bovine granulosa cells. Interestingly, mutations of the putative PKA phosphorylation sites S259, S269 and S275 in USF2 reduced but did not completely abolish transactivation capacity [17]. These findings are nicely complemented by the findings of our study

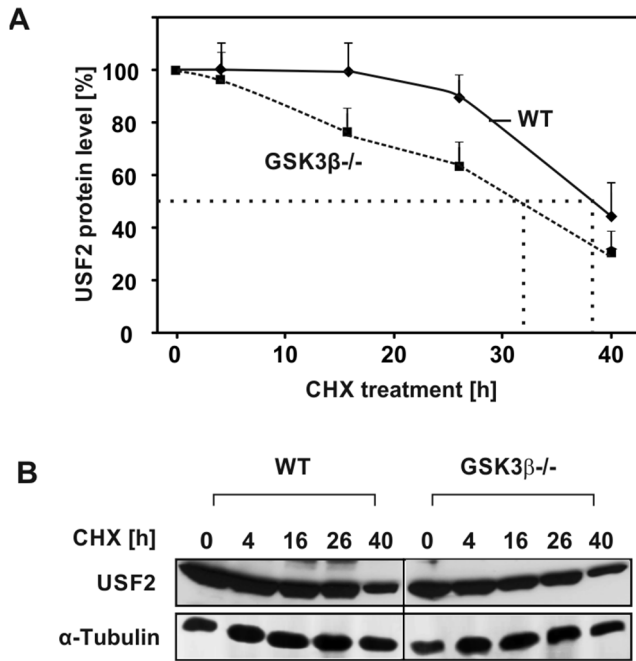


**Figure 6. The half-life of USF2 is induced upon GSK3 $\beta$ -dependent phosphorylation.** (A) GSK3 $\beta$ <sup>+/+</sup> and GSK3 $\beta$ <sup>-/-</sup> cells were treated with 10  $\mu$ g/ml CHX for the indicated time periods. Proteins were isolated, separated by SDS-PAGE and detected by Western blotting. Protein levels were quantified and the relative protein level of USF2 was blotted against the duration of CHX treatment for estimation of the half-life. The dashed line indicates the USF2 half-life where 50% of the USF2 protein level was reached. (B) Representative Western Blot. 50  $\mu$ g of protein from were probed with an antibody against USF2 and  $\alpha$ -tubulin.  
doi:10.1371/journal.pone.0107914.g006

showing that not only PKA but also GSK3 is of importance for the regulation of USF2 DNA binding activity and transactivity. Like in the previous report, our study also showed that mutation of the GSK3 sites in USF2 did not completely abolish its transactivity. This can be explained by the fact that the presence of the transactivation domain alone accounts for a large extend of basal transactivity and that mutation of the phospho-sites only affects the additional increase normally mediated by post-translational phosphorylation. In addition, this view is supported by our data from the structural simulation experiments where the phosphorylation of USF2 by GSK3 only shifts the distance between the two major structural domains but does not alter its overall conformation.

It already has been shown that the protein stability of several proteins which play a role in cancerogenesis is altered upon GSK3 $\beta$ -dependent phosphorylation, among them are for example the transcription factors HIF-1 $\alpha$  [70,71], c-Jun [67], p53 [68] and c-Myb [69], c-Myc [70] and  $\beta$ -catenin [72]. Our study is in line with these findings since cMyc and  $\beta$ -catenin protein levels were found to be enhanced in the GSK3 $\beta$  lacking MEFs (Fig. 3C). In addition, our findings allow adding USF2 to this list of these proteins since our half-life studies revealed that lack of GSK3 $\beta$ -mediated phosphorylation reduces the half-life of USF2. Future experiments need to unravel whether modifications in ubiquitination followed by proteasomal degradation or other mechanisms contribute to this phenomenon.

The induction of USF2 transactivity due to phosphorylation by GSK3 $\beta$  is complemented by the induction in USF2 DNA binding capacity and half-life. At the same time an increased expression of

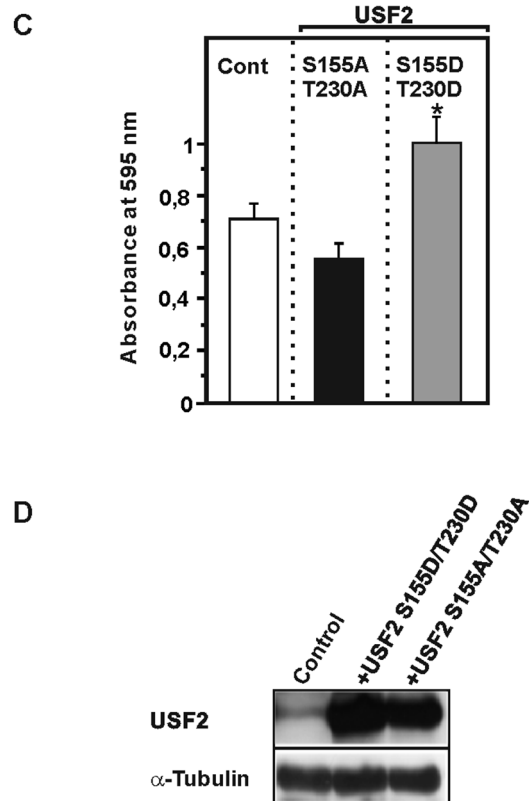
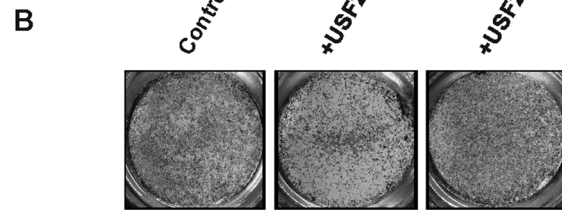
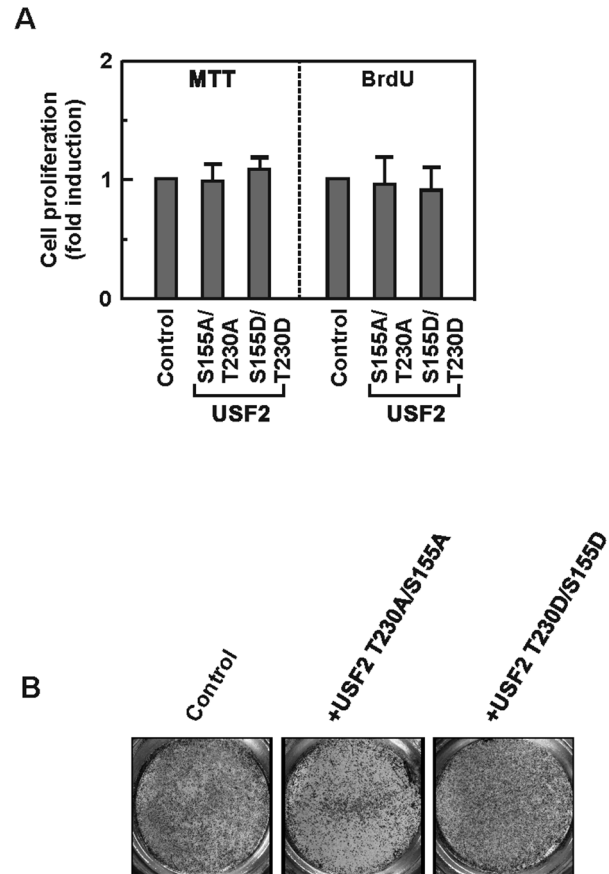


**Figure 7. The phosphorylation of USF2 by GSK3 $\beta$  affects cell migration.** (A, B, C, D) GSK3 $\beta$ <sup>-/-</sup> cells were transfected with vectors allowing expression of USF2-S155A/T230A or USF2-S155D/T230D or an empty vector. Cellular viability, proliferation and cell migration were monitored by MTT, BrdU (A) and cell migration (B, C) assays. (B) Photographs from a representative Transwell chamber experiment. (C) Data represent the absorbance of crystal violet at 595 nm relative to the control. \*, significant difference between GSK3 $\beta$ <sup>-/-</sup> cells and GSK3 $\beta$ <sup>-/-</sup> cells + USF2-S155D/T230D. (D) The expression of USF2 was controlled by Western blotting. 50  $\mu$ g of protein from transfected cells were probed with an antibody against USF2 and  $\alpha$ -tubulin. doi:10.1371/journal.pone.0107914.g007

the USF2 target genes FAS, HO-1, and PAI-1 is initiated. This type of regulation, together with the findings of the migration assay is in line with previous reports indicating that GSK3 $\beta$  and USF2 have a role in cancerogenesis [8,73].

However, the exact function of both, GSK3 $\beta$  and USF2 in cancerogenesis appears to be variable and may depend on the cellular context. While a number of studies support the idea of GSK3 $\beta$  being tumor suppressive, others studies showed that GSK3 $\beta$  may promote cancer development [72]. Similar findings were obtained with respect to USF2; being tumor suppressive with respect to prostate cancer [8,73] but being rather promoting in the development of lung cancer [74] and thyroid cancer [75].

## References

- Corre S, Galibert MD (2005) Upstream stimulating factors: Highly versatile stress-responsive transcription factors. *Pigment Cell Res* 18: 337–348.
- Sirito M, Lin Q, Maity T, Sawadogo M (1994) Ubiquitous expression of the 43- and 44-kDa forms of transcription factor USF in mammalian cells. *Nucleic Acids Res* 22: 427–433.
- Viollet B, Lefrançois-Martinez AM, Henrion A, Kahn A, Raymondjean M, et al (1996) Immunochemical characterization and transacting properties of upstream stimulatory factor isoforms. *J Biol Chem* 271: 1405–1415.
- Gregor PD, Sawadogo M, Roeder RG (1990) The adenovirus major late transcription factor USF is a member of the helix-loop-helix group of regulatory proteins and binds to DNA as a dimer. *Genes Dev* 4: 1730–1740.
- Qyang Y, Luo X, Lu T, Ismail PM, Krylov D, et al (1999) Cell-type-dependent activity of the ubiquitous transcription factor USF in cellular proliferation and transcriptional activation. *Mol Cell Biol* 19: 1508–1517.
- Baxevasis AD, Vinson CR (1993) Interactions of coiled coils in transcription factors: Where is the specificity? *Curr Opin Genet Dev* 3: 278–285.
- Sirito M, Lin Q, Deng JM, Behringer RR, Sawadogo M (1998) Overlapping roles and asymmetrical cross-regulation of the USF proteins in mice. *Proc Natl Acad Sci U S A* 95: 3758–3763.
- Chen N, Szentirmay MN, Pawar SA, Sirito M, Wang J, et al (2006) Tumor-suppression function of transcription factor USF2 in prostate carcinogenesis. *Oncogene* 25: 579–587.
- Ismail PM, Lu T, Sawadogo M (1999) Loss of USF transcriptional activity in breast cancer cell lines. *Oncogene* 18: 5582–5591.
- Chang JT, Yang HT, Wang TC, Cheng AJ (2005) Upstream stimulatory factor (USF) as a transcriptional suppressor of human telomerase reverse transcriptase (hTERT) in oral cancer cells. *Mol Carcinog* 44: 183–192.
- Ocejo-Garcia M, Baokbah TA, Ashurst HL, Cowlshaw D, Soomro I, et al (2005) Roles for USF-2 in lung cancer proliferation and bronchial carcinogenesis. *J Pathol* 206: 151–159.
- Cheung E, Mayr P, Coda-Zabetta F, Woodman PG, Boam DS (1999) DNA-binding activity of the transcription factor upstream stimulatory factor 1 (USF-1) is regulated by cyclin-dependent phosphorylation. *Biochem J* 344 Pt 1: 145–52: 145–152.
- Corre S, Primot A, Baron Y, Le Seyec J, Goding C, et al (2009) Target gene specificity of USF-1 is directed via p38-mediated phosphorylation-dependent acetylation. *J Biol Chem* 284: 18851–18862.
- Galibert MD, Boucontet L, Goding CR, Meo T (1997) Recognition of the E-C4 element from the C4 complement gene promoter by the upstream stimulatory factor-1 transcription factor. *J Immunol* 159: 6176–6183.
- Galibert MD, Carreira S, Goding CR (2001) The usf-1 transcription factor is a novel target for the stress-responsive p38 kinase and mediates UV-induced tyrosinase expression. *EMBO J* 20: 5022–5031.
- Nowak M, Helleboid-Chapman A, Jakel H, Martin G, Duran-Sandoval D, et al (2005) Insulin-mediated down-regulation of apolipoprotein A5 gene expression through the phosphatidylinositol 3-kinase pathway: Role of upstream stimulatory factor. *Mol Cell Biol* 25: 1537–1548.
- Sayasith K, Lussier JG, Siros J (2005) Role of upstream stimulatory factor phosphorylation in the regulation of the prostaglandin G/H synthase-2 promoter in granulosa cells. *J Biol Chem* 280: 28885–28893.
- Terragni J, Nayak G, Banerjee S, Medrano JL, Graham JR, et al (2011) The E-box binding factors max/mnt, MITF, and USF1 act coordinately with FoxO to regulate expression of proapoptotic and cell cycle control genes by phosphatidylinositol 3-kinase/akt/glycogen synthase kinase 3 signaling. *J Biol Chem* 286: 36215–36227.
- Xiao Q, Kenessey A, Ojamaa K (2002) Role of USF1 phosphorylation on cardiac alpha-myosin heavy chain promoter activity. *Am J Physiol Heart Circ Physiol* 283: H213–H219.
- Wong RH, Chang I, Hudak CS, Hyun S, Kwan HY, et al (2009) A role of DNA-PK for the metabolic gene regulation in response to insulin. *Cell* 136: 1056–1072.
- Dimova EY, Kietzmann T (2006) Cell type-dependent regulation of the hypoxia-responsive plasminogen activator inhibitor-1 gene by upstream stimulatory factor-2. *J Biol Chem* 281: 2999–3005.
- Cohen P, Frame S (2001) The renaissance of GSK3. *Nat Rev Mol Cell Biol* 2: 769–776.
- Frame S, Cohen P (2001) GSK3 takes centre stage more than 20 years after its discovery. *Biochem J* 359: 1–16.
- Jope RS, Johnson GV (2004) The glamour and gloom of glycogen synthase kinase-3. *Trends Biochem Sci* 29: 95–102.
- Patel S, Doble B, Woodgett JR (2004) Glycogen synthase kinase-3 in insulin and wnt signalling: A double-edged sword? *Biochem Soc Trans* 32: 803–808.
- Darrington RS, Campa VM, Walker MM, Bengoa-Vergnioun N, Gorrone-Etxebarria I, et al (2012) Distinct expression and activity of GSK-3 and GSK-3 in prostate cancer. *International Journal of Cancer* 131: E872–E883.
- Mulholland DJ, Dedhar S, Wu H, Nelson CC (2006) PTEN and GSK3: Key regulators of progression to androgen-independent prostate cancer. *Oncogene* 25: 329–337.
- Fiol CJ, Wang A, Roeske RW, Roach PJ (1990) Ordered multisite protein phosphorylation. analysis of glycogen synthase kinase 3 action using model peptide substrates. *The Journal of biological chemistry* 265: 6061–6065.
- Lefrançois-Martinez AM, Martínez A, Antoine B, Raymondjean M, Kahn A (1995) Upstream stimulatory factor proteins are major components of the glucose response complex of the L-type pyruvate kinase gene promoter. *J Biol Chem* 270: 2640–2643.
- Sadowski I, Ptashne M (1989) A vector for expressing GAL4(1-147) fusions in mammalian cells. *Nucleic Acids Res* 17.
- He X, Saint-Jeannet J, Woodgett JR, Varmus HE, Dawid IB (1995) Glycogen synthase kinase-3 and dorsoventral patterning in xenopus embryos. *Nature* 374: 617–622.
- Stambolic V, Woodgett JR (1994) Mitogen inactivation of glycogen synthase kinase-3 beta in intact cells via serine 9 phosphorylation. *Biochem J* 303 (Pt 3): 701–704.
- Hill-Kapturczak N, Sikorski E, Voakes C, Garcia J, Nick HS, et al (2003) An internal enhancer regulates heme- and cadmium-mediated induction of human

Although no study has yet correlated the activity of GSK3 $\beta$  with the activity of USF2 in a certain tumor setting, the findings of the present study would favor the tumor promoting aspects of GSK3 $\beta$  and USF2 since GSK3 $\beta$  activated USF2 enhanced cell migration which may be important in terms of tumor cell metastasis. In addition, cross-talk(s) between signalling pathways depending on different growth conditions, the cellular context and/or tissue-specific aspects may well be other player(s) influencing the activity of USF2.

In summary, our study identified GSK3 $\beta$  as a kinase that phosphorylates USF2 and thereby regulates its function. The GSK3 $\beta$ -mediated phosphorylation of USF2 at S155 and at T230 leads to increased transactivity, DNA-binding, and half-life of the transcription factor and to an induction of cell migration. These novel findings on the regulation of the transcription factor USF2 set the basis for further studies investigating how these mechanisms contribute to the development of different types of cancer.

## Author Contributions

Conceived and designed the experiments: TH EYD AHJ TK. Performed the experiments: TH TFC CG EYD SS. Analyzed the data: TH TFC CG EYD AHJ TK. Contributed reagents/materials/analysis tools: AHJ TK. Contributed to the writing of the manuscript: TH CG SS AHJ EYD TK.

- heme oxygenase-1. *American journal of physiology. Renal physiology* 285: F515–523.
34. Dimova EY, Moller U, Herzig S, Fink T, Zachar V, et al (2005) Transcriptional regulation of plasminogen activator inhibitor-1 expression by insulin-like growth factor-1 via MAP kinases and hypoxia-inducible factor-1 in HepG2 cells. *Thromb Haemostasis* 93: 1176–1184.
  35. Kim JB, Sarraf P, Wright M, Yao KM, Mueller E, et al (1998) Nutritional and insulin regulation of fatty acid synthetase and leptin gene expression through ADD1/SREBP1. *J Clin Invest* 101: 1–9.
  36. Hoeflich KP, Luo J, Rubie EA, Tsao MS, Jin O, et al (2000) Requirement for glycogen synthase kinase-3 $\beta$  in cell survival and NF- $\kappa$ B activation. *Nature* 406: 86–90.
  37. Jordan M, Schallhorn A, Wurm FM (1996) Transfecting mammalian cells: Optimization of critical parameters affecting calcium-phosphate precipitate formation. *Nucleic Acids Res* 24: 596–601.
  38. Immenschuh S, Hinke V, Ohlmann A, Gifhorn-Katz S, Katz N, et al (1998) Transcriptional activation of the haem oxygenase-1 gene by cGMP via a cAMP response element/activator protein-1 element in primary cultures of rat hepatocytes. *Biochem J* 334 (Pt 1): 141–146.
  39. Samoylenko A, Dimova EY, Horbach T, Teplyuk N, Immenschuh S, et al (2008) Opposite expression of the antioxidant heme oxygenase-1 in primary cells and tumor cells: Regulation by interaction of USF-2 and fra-1. *Antioxidants & redox signaling* 10: 1163–1174.
  40. Livak KJ, Schmittgen TD (2001) Analysis of relative gene expression data using real-time quantitative PCR and the 2(-delta delta C(T)) method. *Methods* 25: 402–408.
  41. Ganjam GK, Dimova EY, Unterman TG, Kietzmann T (2009) FoxO1 and HNF-4 are involved in regulation of hepatic glucokinase gene expression by resveratrol. *J Biol Chem* 284: 30783–30797.
  42. Shevchenko A, Wilm M, Vorm O, Mann M (1996) Mass spectrometric sequencing of proteins silver-stained polyacrylamide gels. *Anal Chem* 68: 850–858.
  43. Liu Q, Berchner-Pfannschmidt U, Moller U, Brecht M, Wotzlaw C, et al (2004) A fenton reaction at the endoplasmic reticulum is involved in the redox control of hypoxia-inducible gene expression. *Proc Natl Acad Sci U S A* 101: 4302–4307.
  44. Nelson JD, Denisenko O, Bomszyk K (2006) Protocol for the fast chromatin immunoprecipitation (ChIP) method. *Nature protocols* 1: 179–185.
  45. Fujii-Yamamoto H, Kim JM, Arai K, Masai H (2005) Cell cycle and developmental regulations of replication factors in mouse embryonic stem cells. *J Biol Chem* 280: 12976–12987.
  46. Zhang Y (2008) I-TASSER server for protein 3D structure prediction. *BMC Bioinformatics* 9: 40-2105-9-40.
  47. Roy A, Kucukural A, Zhang Y (2010) I-TASSER: A unified platform for automated protein structure and function prediction. *Nat Protoc* 5: 725–738.
  48. Pronk S, Pall S, Schulz R, Larsson P, Bjelkmar P, et al (2013) GROMACS 4.5: A high-throughput and highly parallel open source molecular simulation toolkit. *Bioinformatics* 29: 845–854.
  49. van Gunsteren WF, Billeter SR, Eising AA, Hunenberger PH, Kruger P, et al (1996) Biomolecular simulation: The GROMOS96 manual and user guide. Zurich, Switzerland: Vdf Hochschulverlag AG an der ETH Zurich. 1042 p.
  50. Humphrey W, Dalke A, Schulten K (1996) VMD: Visual molecular dynamics. *J Mol Graph* 14: 33–38, 27–28.
  51. Berendsen HJC, Postma JPM, van Gunsteren WF, Hermans J (1981) Interaction models for water in relation to protein hydration. In: Anonymous Dordrecht: D. Reidel. 331–342.
  52. Parrinello M (1981) Polymorphic transitions in single crystals: A new molecular dynamics method. *J Appl Phys* 52.
  53. Bussi G, Donadio D, Parrinello M (2007) Canonical sampling through velocity rescaling. *J Chem Phys* 126.
  54. Darden T, York D, Pedersen L (1993) Particle mesh ewald: An N<sup>2</sup>log(N) method for ewald sums in large systems. *J Chem Phys* 98.
  55. Miyamoto S, Kollman PA (1992) Settle: An analytical version of the SHAKE and RATTLE algorithm for rigid water models. *Journal of Computational Chemistry* 13: 952–962.
  56. Sutherland C (2011) What are the bona fide GSK3 substrates? *Int J Alzheimers Dis* 2011: 505607.
  57. Nupponen NN, Kakkola L, Koivisto P, Visakorpi T (1998) Genetic alterations in hormone-refractory recurrent prostate carcinomas. *Am J Pathol* 153: 141–148.
  58. Groenen PM, Garcia E, Debeer P, Devriendt K, Fryns JP, et al (1996) Structure, sequence, and chromosome 19 localization of human USF2 and its rearrangement in a patient with multicystic renal dysplasia. *Genomics* 38: 141–148.
  59. Astbury C, Jackson-Cook CK, Culp SH, Paisley TE, Ware JL (2001) Suppression of tumorigenicity in the human prostate cancer cell line M12 via microcell-mediated restoration of chromosome 19. *Genes Chromosomes Cancer* 31: 143–155.
  60. Christensen LL, Tobiasen H, Holm A, Schepeler T, Ostenfeld MS, et al (2012) miRNA-362-3p induces cell cycle arrest through targeting of E2F1, USF2 and PTPN1 and is associated with recurrence of colorectal cancer. *International journal of cancer. Journal international du cancer*.
  61. Davis PL, Miron A, Andersen LM, Iglehart JD, Marks JR (1999) Isolation and initial characterization of the BRCA2 promoter. *Oncogene* 18: 6000–6012.
  62. Reisman D, Rotter V (1993) The helix-loop-helix containing transcription factor USF binds to and transactivates the promoter of the p53 tumor suppressor gene. *Nucleic Acids Res* 21: 345–350.
  63. Jaiswal AS, Narayan S (2001) Upstream stimulating factor-1 (USF1) and USF2 bind to and activate the promoter of the adenomatous polyposis coli (APC) tumor suppressor gene. *J Cell Biochem* 81: 262–277.
  64. Samoylenko A, Roth U, Jungermann K, Kietzmann T (2001) The upstream stimulatory factor-2a inhibits plasminogen activator inhibitor-1 gene expression by binding to a promoter element adjacent to the hypoxia-inducible factor-1 binding site. *Blood* 97: 2657–2666.
  65. Luo X, Sawadogo M (1996) Functional domains of the transcription factor USF2: Atypical nuclear localization signals and context-dependent transcriptional activation domains. *Mol Cell Biol* 16: 1367–1375.
  66. Luo X, Sawadogo M (1996) Antiproliferative properties of the USF family of helix-loop-helix transcription factors. *Proc Natl Acad Sci U S A* 93: 1308–1313.
  67. Chen B, Huang C, Chang W, Chen Y, Kikkawa U, et al (2007) PP2B-mediated dephosphorylation of c-jun C terminus regulates phorbol ester-induced c-jun/Sp1 interaction in A431 cells. *Mol Biol Cell* 18: 1118–1127.
  68. Qu L, Huang S, Baltzis D, Rivas-Estilla A, Pluquet O, et al (2004) Endoplasmic reticulum stress induces p53 cytoplasmic localization and prevents p53-dependent apoptosis by a pathway involving glycogen synthase kinase-3 $\beta$ . *Genes Dev* 18: 261–277.
  69. Kitagawa K, Hiramatsu Y, Uchida C, Isobe T, Hattori T, et al (2009) Fbw7 promotes ubiquitin-dependent degradation of c-myc: Involvement of GSK3-mediated phosphorylation of thr-572 in mouse c-myc. *Oncogene* 28: 2393–2405.
  70. Flugel D, Grolach A, Michiels C, Kietzmann T (2007) Glycogen synthase kinase 3 phosphorylates hypoxia-inducible factor 1 $\alpha$  and mediates its destabilization in a VHL-independent manner. *Mol Cell Biol* 27: 3253–3265.
  71. Flugel D, Grolach A, Kietzmann T (2012) GSK-3 $\beta$  regulates cell growth, migration, and angiogenesis via Fbw7 and USP28-dependent degradation of HIF-1 $\alpha$ . *Blood* 119: 1292–1301.
  72. Aberle H, Bauer A, Stappert J, Kispert A, Kemler R (1997) Beta-catenin is a target for the ubiquitin-proteasome pathway. *EMBO J* 16: 3797–3804.
  73. Luo X, Sawadogo M (1996) Antiproliferative properties of the USF family of helix-loop-helix transcription factors. *Proc Natl Acad Sci U S A* 93: 1308–1313.
  74. Ocejio-Garcia M, Baokbah TAS, Ashurst HL, Cowlishaw D, Soomro I, et al (2005) Roles for USF-2 in lung cancer proliferation and bronchial carcinogenesis. *J Pathol* 206: 151–159.
  75. Landa I, Ruiz-Llorente S, Montero-Conde C, Inglada-Perez L, Schiavi F, et al (2009) The variant rs1867277 in FOXE1 gene confers thyroid cancer susceptibility through the recruitment of USF1/USF2 transcription factors. *PLoS Genet* 5: e1000637.